**Transactions of JASCOME Vol. 17 (16 December, 2017), Paper No. 22-171215** JASCOME

# Quantum scattering theory and stealth finite element analysis

Sathwik Bharadwaj,[1] Andrei Ilyashenko,[2] A. Gianfrancesco,[2] and L. R. Ram-Mohan[3]

1) Department of Physics, Worcester Polytechnic Institute(100 Institute Rd, Worcester, MA, 01609, E-mail: sathwik@wpi.edu).

2) Department of Physics, Worcester Polytechnic Institute(100 Institute Rd, Worcester, MA, 01609).

3) Departments of Physics, Electrical and Computer Engineering, and Mechanical Engineering, Worcester Polytechnic Institute (100 Institute Rd, Worcester, MA, 01609, E-mail: lrram@wpi.edu).

We develop a novel method based on finite element analysis (FEA) to examine scattering in finite, nanoscale systems. The essential Cauchy (mixed) boundary conditions (BCs) needed in scattering are reduced to simpler Dirichlet BCs by introducing totally absorbing elements, or "stealth elements," whose material properties are optimized to give decaying solutions vanishing at the boundaries. Schrödinger equation with a source term is discretized using the principle of stationary action to obtain highly accurate numerical near field solutions. This approach provides excellent results for both open domains, as well as with confined geometries. In 1D, we provide concrete examples and demonstrate the high accuracy of this method. In 2D confined waveguides, we obtain scattered wavefunctions for geometrically complex scattering centers, and multiple scattering that go beyond the traditional perturbative and far field approximations. The modal analysis of reflected and transmitted waves allows us to obtain transmission coefficients for both propagating and evanescent modes.

***Key Words***: *scattering theory, finite element analysis, stealth elements*

## 1. Introduction

In physics, scattering is a general phenomenon which is of considerable interest from classical mechanics to relativistic field theory.(1) Many of the early understanding of quantum mechanics pioneered from scattering and collision experiments.(2) Typically, in low energy quantum scattering problems, we consider an incoming wave with known energy, scattering amplitudes and cross-sections are determined in the asymptotic limit.(3) However, in finite nanoscale systems, there is an urgency to understand near field scattering behavior for several applications such as semiconductor resonant tunneling heterostructures, quantum cascade lasers, scanning tunneling microscopy, tunneling resistance devices and split-gate narrow channel MOSFETs.

Finite element analysis (FEA) is a generalized variational approach in which we discretize the action integral to obtain accurate numerical solutions.(4) The mixed (Cauchy) boundary conditions (BCs) are crucial while using the principle of stationary action to solve for scattering problems within the variational approach. In general, the mixed BCs are difficult to implement in open domains and, for that matter even in confined geometries, in 2D and 3D systems. In open domains, the scattered wave is represented in terms of outgoing Hankel functions. The fact that the Hankel functions of all orders have the same asymptotic behavior allows a substantial simplification in BCs. However, in considering finite domain systems, this traditional procedure of applying BCs requires a re-examination since we do not have an asymptotic limit as the active region is geometrically constrained. Here we show that the use of absorbing material around the scattering (active) region provides a unique way of reducing the mixed BCs to much simpler Dirichlet BCs. The absorbing finite elements, which we call "stealth elements", have material properties modified so as to provide damping of the waves that impinge on them, with no reflection. The concept of stealth elements draws on the idea of "perfectly matched layers" used in electromagnetic (EM) scattering,(5) where we allow the dielectric constant to be complex and vary its value smoothly within each layer. In our case, we instead consider a smoothly varying complex mass within stealth elements. In the active region, we consider an electron antenna which is provided by introducing a source term to the Schrödinger equation.

In Sec. 2, we first discuss the mixed BCs in typical 1D scattering problems and then show the method of reducing mixed BCs to Dirichlet BCs, by introducing stealth elements. In Sec. 3, we define the Schrödinger equation with

Received: 26 Sept., 2017, Accepted: 6 Nov., 2017

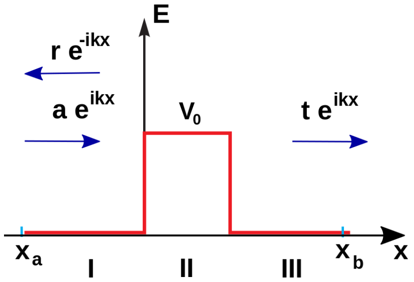


Fig. 1: Scattering through a 1D barrier of height $V_0$. We consider an incoming plan wave with an amplitude $a$ and the energy $E$. The corresponding wavevector is $k = \sqrt{2m^* E/\hbar^2}$. Here, $r$ and $t$ are the reflection and transmission amplitudes, respectively.

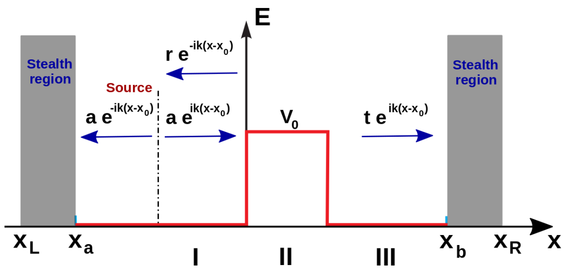


Fig. 2: Scattering through a 1D barrier of height $V_0$ with stealth region on either side of the barrier. We consider a source at $x = x_0$ within the active region which injects an incoming wave with an amplitude $a$ and the energy $E$ in both directions. The corresponding wavevector is $k = \sqrt{2m^* E/\hbar^2}$. Here, $r$ and $t$ are the reflection and transmission coefficients respectively.

a source term and obtain the source parameter using the Green's function technique. We discuss the finite element method for scattering in Sec. 4. In Sec. 5, we extend our formalism to study electron scattering from both repulsive and attractive scatterers in a 2D waveguide. Conclusions and future research directions are presented in Sec. 6.

## 2. Boundary conditions for scattering

We first briefly discuss the boundary conditions in a traditional 1D barrier scattering. In Fig. 1, we consider an incoming plane wave from a source at $x = -\infty$ with a given energy $E$ and an amplitude $a$. The total wavefunction in region I and III are given by

$$\begin{aligned} \psi_I &= a e^{ikx} + r\, e^{-ikx}, \\ \psi_{III} &= t e^{ikx}, \end{aligned} \tag{1}$$

where, the wavevector $k = \sqrt{2m^* E/\hbar^2}$ and $m^*$ is the effective mass of an electron. Hence we obtain Cauchy BCs at $x_a$ and $x_b$ given by

$$\begin{aligned} \left[\frac{d\psi_I(x)}{dx} + ik\psi_I(x)\right]_{x=x_a} &= 2ika e^{ikx}\Big|_{x=x_a}, \\ \left[\frac{d\psi_{III}(x)}{dx} - ik\psi_{III}(x)\right]_{x=x_b} &= 0. \end{aligned} \tag{2}$$

We reduce the above mixed BCs to simpler Dirichlet BCs by creating absorbers on either side of the barrier (see Fig. 2). We optimize the parameters within these absorbers in such a way that there is no reflection from any wave incident on them. We consider a complex electron effective mass $\overline{m} = m^* \left(1 + i\ \alpha(x)\right)$, where, $\alpha(x)$ is a cubic Hermite interpolation polynomial which varies smoothly from 0 to $\alpha_{max}$ within the stealth region and equal to 0 in the active region. Let $\alpha(x_a) = \alpha(x_b) = 0$ and, $\alpha(x_L) = \alpha(x_R) = \alpha_{max}$ (see Fig. 2). The wave equation within stealth regions is given by

$$\frac{d}{dx}\left(\frac{1}{(1+i\alpha(x))}\frac{d}{dx}\psi(x)\right) + k^2(1+i\alpha(x))\psi(x) = 0. \tag{3}$$

Solutions to the above equation will have highly damped behavior due to suitably chosen $\alpha(x)$. Hence we apply Dirichlet BCs that are given by $\psi(x_L) = \psi(x_R) = 0$. In Appendix A, we derive the condition for no reflection at the stealth interface and justify the choice for $\alpha(x)$ to be a smooth function.

## 3. Schrödinger equation with a source term

In the previous section, we created totally absorbing stealth regions around the scattering center. Hence, we require an electron antenna (source) which can inject plane waves of given energy ($E$) and amplitude ($a$). The Schrödinger equation in the active region with a source term is given by

$$\left[-\frac{d}{dx}\left(\frac{\hbar^2}{2m^*}\frac{d}{dx}\right) + V(x) - E\right]\psi(x) = -S\frac{\hbar^2}{2m^*}\delta(x - x_0), \tag{4}$$

where, $x_0$ is the location of a source within the active region and $S$ is the source parameter. In the absence of any potential, the equation for Green's function $G(x - x_0)$ in the active region is given by

$$\left[-\frac{d}{dx}\left(\frac{\hbar^2}{2m^*}\frac{d}{dx}\right) - E\right] G(x-x_0) = -S\ \frac{\hbar^2}{2m^*}\ \delta(x-x_0). \tag{5}$$

The Fourier transform of $G(x - x_0)$ is given by

$$G(x - x_0) = \frac{1}{2\pi}\int_{-\infty}^{\infty} dk'\ g(k')\ \exp(ik'(x - x_0)). \tag{6}$$

Substituting Eq. (6) in Eq. (5) and representing the $\delta$ function in the Fourier space we obtain

$$g(k') = -\frac{S}{2k}\left[\frac{1}{k'-k} - \frac{1}{k'+k}\right]. \tag{7}$$

By using the inverse Fourier transformation and contour integration techniques we obtain

$$G(x - x_0) = \frac{S}{2ik}\begin{cases} \exp(ik(x - x_0)), & x > x_0; \\ \exp(-ik(x - x_0)), & x < x_0. \end{cases} \tag{8}$$

Hence, we identify the source parameter as $S = 2ika$, to obtain plane waves with a specified amplitude $a$ and wavevector $k$.

Table 1: We compare the analytically and numerically obtained transmission coefficients ($T$) for a barrier of width = 40Å. Here, stealth region width = 50Å, incoming wave amplitude, $a = 1$ and the source antenna is located at $-40$Å. Number of elements = 1000. We employ the quintic Hermite interpolation polynomials. Effective mass of conduction electron in GaAs, $m^* = 0.067 m_e$ is considered ($m_e$ is the mass of an electron).

| Barrier Height (ev) | Incoming energy(ev) | T (Analytical) | T (Numerical) |
|---|---|---|---|
| 0.5 | 0.5 | 0.53212186 | 0.53211017 |
| 0.5 | 1.0 | 0.89786166 | 0.89786127 |
| 0.5 | 2.0 | 0.99976389 | 0.99967599 |

## 4. Finite element analysis for scattering

The action integral corresponding to Eq. (3) and Eq. (4) is given by

$$\mathcal{A}/T = \int_{x_L}^{x_R} dx\, \frac{\partial \psi^*(x)}{\partial x} \cdot \frac{1}{(1+\alpha(x))} \frac{\partial \psi(x)}{\partial x} + \psi^* \left[ \frac{2m^*}{\hbar^2} \left[ V(x) - E\,(1 + i\alpha(x)) \right] \right] \psi(x) + \int_{x_L}^{x_R} dx\; \psi^*(x)\, S\, \delta(x - x_0), \tag{9}$$

where, $\alpha(x)$ is equal to 0 in the active region. We are solving here the time-independent problem so that the time integral over the range $[0, T]$ in the action is simply $T$. Dirichlet BCs are implemented at $x = x_L$ and $x = x_R$. Discretization of the above action integral within finite element framework and variation with respect to $\psi^*$ provides us the total wavefunction throughout. In Table 1, we compare the transmission coefficients obtained through our analysis and well known analytical calculations for scattering from a 1D barrier potential in GaAs. We achieve an accuracy of $\sim 10^{-4}$. We can systematically increase the accuracy through mesh size refinement ($h$-refinement), or by the use of higher order interpolation polynomials ($p$-refinement) for convergence within the FEA.

Next, we consider the case of electron scattering through a 1D double barrier potential in GaAs. In Fig. 3, we plot the first above-barrier resonant state in a double barrier of height 0.3eV. Notice that within stealth regions (shaded regions) the wavefunction decay smoothly to zero. In Fig. 4, we see that for the above barrier states, resonance occurs as doublets which correspond to the confinement above each of the barrier. Three resonant states below the barrier height (0.3 eV) corresponds to electrons reasonably trapped within the well between the two barriers.

## 5. Scattering in 2D waveguides

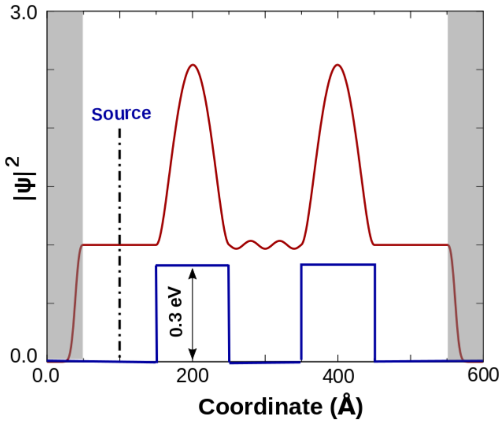


Fig. 3: Probability distribution for the first above-barrier resonant state with incoming energy 0.355eV is shown. The source is located at 100 Å. The stealth region is shaded in gray and the width of the stealth region is equal to 50 Å.

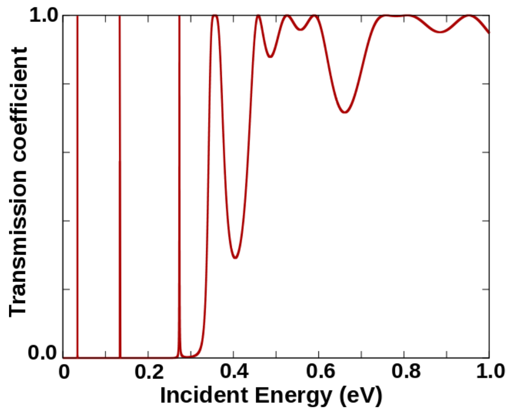


Fig. 4: We have plotted the transmission coefficient as a function of energy for a double barrier potential. Each of the barriers is of height 0.3eV with a width of 100Å and are 100Å apart.

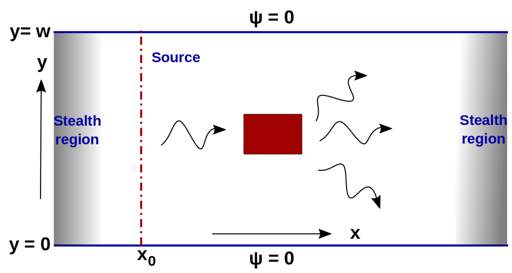


Fig. 5: We show a schematic picture of scattering in a 2D waveguide of width $w$. We place the stealth region at either end of the waveguide. The wave propagation is along the $x$-axis.

Let us consider a 2D waveguide of width $w$ with wave propagation along the $x$-axis (see Fig. 5). We include the stealth region at either end of the waveguide and a source in the active region at $x = x_0$. Particles are confined in the transverse direction. Hence, we obtain the solutions, in the

$y$ direction of the infinite potential well of width $w$. Thus the total incident energy as a sum of the energies in $x$ and $y$ directions is given by

$$E_n = E_{x,n} + \frac{n^2\pi^2\hbar^2}{2m^* w^2}, \quad (10)$$

where $n$ is the incoming integer mode number. We refer to $E_{y,n} = n^2\pi^2\hbar^2/2m^*w^2$ as the subband minimum of the mode $n$. The corresponding dispersion relation is given by

$$k^2 = k_{xn}^2 + \frac{n^2\pi^2}{w^2}, \quad (11)$$

where $k_{xn}$ is the wavevector and $a_n$ is the specified amplitude of the incoming plane wave in the mode $n$. The set of propagating wavefunctions for an empty waveguide with a source at $x_0$ is given by

$$\left\{\phi_m^{\pm}(x,y) = \exp(\pm i k_{xm}\,|x-x_0|)\sin\left(\frac{m\pi y}{w}\right)\Big|\, m\in\mathbb{N}\right\}. \quad (12)$$

If we consider a scatterer centered at origin, the set of different possible evanescent modes is given by

$$\left\{\tilde{\phi}_m^{\pm}(x,y) = \exp(\pm K_{xm}\;x)\sin\left(\frac{m\pi y}{w}\right)\Big|\, m\in\mathbb{N}\right\}, \quad (13)$$

where $K_{xm} = \sqrt{m^2\pi^2/w^2 - k^2}$ represents the evanescent wavevector. For a specified mode $n$ and an amplitude $a_n$, the incoming wave from the source is given by

$$\psi_n(x,y) = \begin{cases} a_n\,\phi_n^+(x,y), & x > x_0; \\ a_n\,\phi_n^-(x,y), & x < x_0. \end{cases} \quad (14)$$

The transmitted and reflected waves are given by

$$\psi_t(x,y) = \sum_{\substack{m=1 \\ k\geq n\pi/w}} t_{nm}\phi_m^+(x,y) + \sum_{\substack{m \\ k< n\pi/w}} \tilde{t}_{nm}\tilde{\phi}_m^-(x,y),$$
$$\psi_r(x,y) = \sum_{\substack{m=1 \\ k\geq n\pi/w}} r_{nm}\phi_m^-(x,y) + \sum_{\substack{m \\ k< n\pi/w}} \tilde{r}_{nm}\tilde{\phi}_m^+(x,y), \quad (15)$$

where $t_{nm}$ and $r_{nm}$ are the transmission and reflection amplitudes for the propagating modes and, $\tilde{t}_{nm}$ and $\tilde{r}_{nm}$ are the transmission and reflection amplitudes for the evanescent modes, respectively. In our analysis we obtain the total wavefunction which includes both propagating and evanescent contributions throughout. We determine the transmission and reflection coefficients using the orthogonality of sine functions at a fixed $x = x'$. For example,

$$t_{nm} = \int_0^w dy\;\left[\phi_m^+(x',y)\right]^* \cdot \psi_t(x',y). \quad (16)$$

We carry out this integration on either side at an equal horizontal distance ($l$) away from the scattering center. The transmission coefficient ($T_{nm}$) for a propagating mode $m$ is defined as a ratio of the outgoing mode current ($J_{nm}$) to the incoming current ($J_{in}$). Hence

$$T_{nm} = \frac{J_{nm}}{J_{in}} = \frac{k_{xm}\,|t_{nm}|^2}{k_{xn}a_n^2}. \quad (17)$$

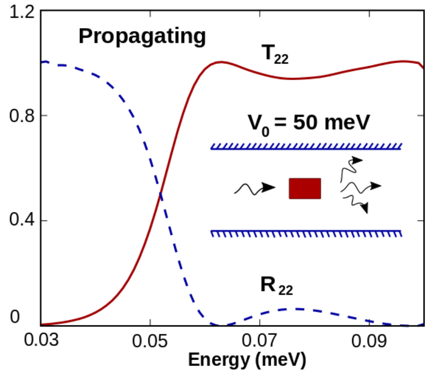

Fig. 6: The transmission ($T_{22}$) and reflection ($R_{22}$) coefficients are shown as a function of energy for the propagating mode $n = 2$, with an incoming wave from the same mode for scattering through a rectangular potential of dimensions 150Å × 200Å and height 50 meV.

The evanescent waves will not contribute to the current since they are real functions. Hence, for a given length $l$ away from the scattering center we define

$$\tilde{T}_{nm}(l) = \frac{\tilde{t}_{nm}^2\;\exp\left(-2K_{xm}l\right)}{a_n^2}, \quad (18)$$

as the transmission coefficient for the evanescent mode $m$. In a similar manner, we can determine the reflection coefficients $R_{nk}$ and $\tilde{R}_{nk}$ for the propagating and evanescent reflected modes respectively. The conservation of probability current requires that

$$\sum_{\substack{m \\ k\geq n\pi/w}} \left(\,T_{nm} + R_{nm}\,\right) = 1. \quad (19)$$

As a prototypical example, we consider a 2D GaAs waveguide of width 300Å. For this waveguide, the subband minima are given by, $E_{y,1} = 6.24$ meV, $E_{y,2} = 24.95$ meV, $E_{y,3} = 56.14$ meV, $E_{y,4} = 99.80$ meV and $E_{y,5} = 155.94$ meV. As a first example, we consider scattering of the conduction electrons through a single rectangular potential of dimensions 150Å × 200Å and height 50 meV. We consider an incoming wave coming with mode $n = 2$. In Fig. 6, we plot $T_{22}$ and $R_{22}$ coefficients as a function of energy. We see that the transmission (reflection) probability slowly increases (decreases) and reaches a resonance. In Fig. 7, we observe that the evanescent states associated with the mode 4 slowly increases and reaches a maximum at $E_{y,4}$.[6] Evanescent modes contribute fairly symmetrically for both transmitted and reflected waves.

Our analysis can be easily extended to study multiple scattering problems. We consider a system of three circular holes of radius 30Å aligned vertically at $x = 0$. We consider that within each hole, we have a constant potential, $V_0 = -50$ meV. In Fig. 8, we see that the transmission

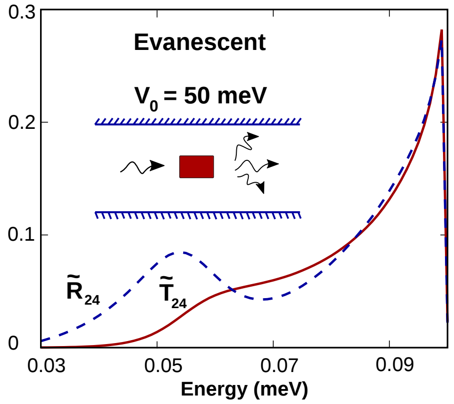


Fig. 7: The transmission ($\tilde{T}_{24}$) and reflection ($\tilde{R}_{24}$) coefficients are shown as a function of energy for the evanescent waves associated with mode $n = 4$, with an incoming wave from the mode $n = 2$ at a distance $l = 50$Å, for scattering through a rectangular potential of dimensions 150Å × 200Å and height 50 meV. We observe that the amplitude will reach a maximum at the 4th subband minimum with energy $E_{y,4} = 99.80$ meV.

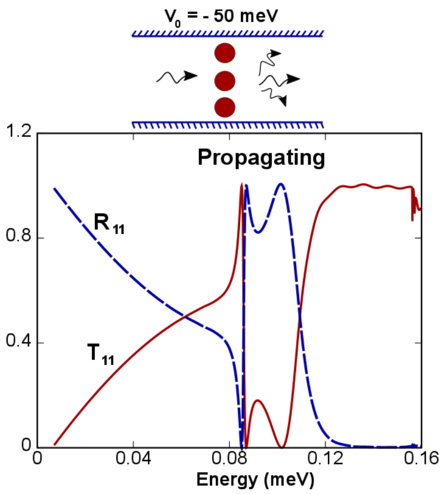


Fig. 8: The transmission ($T_{11}$) and reflection ($R_{11}$) coefficients are shown as a function of energy for the propagating mode $n = 1$, with an incoming wave from the same mode for scattering through vertically aligned three circular holes of radius 30Å whose centers are 100Å apart, and depth −50 meV.

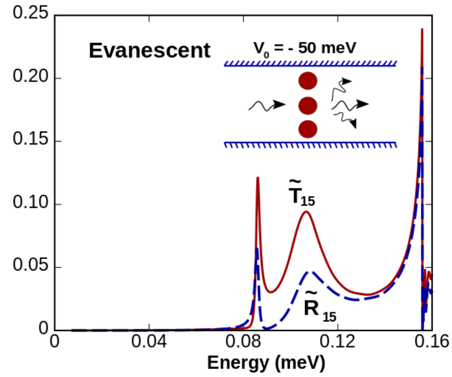


Fig. 9: The transmission ($\tilde{T}_{15}$) and reflection ($\tilde{R}_{15}$) coefficients are shown as a function of energy for the evanescent mode $n = 5$, with an incoming wave from the mode 1 at a distance $l = 50$Å, for scattering through vertically aligned three circular holes of radius 30Å whose centers are 100Å apart, and depth −50 meV.

and reflection coefficients exhibit well known Fano profiles.[7] More intriguing is that even the evanescent modes reveal a similar Fano profile due to coupling between bound states of the holes with scattered evanescent states (see Fig. 9).

## 6. Conclusions

A typical text-book treatment of scattering involves an incoming prepared state from $x = -\infty$, and cross-sections are obtained by applying BCs in the asymptotic limit. In finite, nano-scale systems it is necessary to obtain solutions within a few wavelengths away from the scattering center. Using the stealth elements, we have redefined the quantum scattering problem with "sources and absorbers." In summery, we have shown that

1. the quantum scattering can be brought into the variational framework using the action integral formalism.
2. the use of stealth elements reduces the Cauchy BCs to simpler Dirichlet BCs at the periphery. In this way we substantially reduce the computational complexity. The parameter, $\alpha$, is varied smoothly in the stealth region as a function of coordinates $\boldsymbol{r}$ for each energy $E$ to ensure no reflection at the stealth interface.
3. Schrödinger equation with a source term provides a way of designing a carrier antenna in the active region which inject the plane waves of a specified energy and amplitude while the active region is enclosed by absorbers.
4. the FEA provides a natural way of handling geometrically complex potentials and multiple scattering in any dimension.

In confined geometries, the total wavefunction obtained through our analysis includes the contribution from evanescent modes. In 2D or 3D open domains, the stealth elements are placed around the scattering center in all directions and the source is located in the active region. Our calculations are in progress.

## 7. Acknowledgments

We thank the Center for Computational NanoScience (CCNS) at WPI for the computational resources used for these calculations.

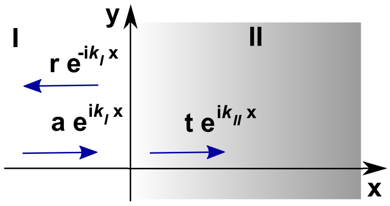


Fig. 10: We have shown the transmission and reflection at the stealth region interface. Here, $k_I$ and $k_{II}$ are the corresponding wavevectors in the regions I and II, respectively. Here, $a$, $r$ and $t$ are the incident, reflected and transmitted amplitudes, respectively.

## Appendix A: No reflection condition at the stealth interface

We need to ensure that there is no reflection from a wave incident on the stealth interface. Let us consider that in 1D we have a stealth interface at $x = 0$. In region I, $(x < 0)$ we have an incoming wave of an amplitude $a$ and energy $E$ that emerged from a source at $x = -\infty$. The region II, $(x > 0)$ is filled with stealth finite elements. In general there will be both reflection and transmission at any interface. To begin with we consider a uniform stealth region. Let the electron effective mass in region II be given by $\overline{m} = m^*(1 + i\ \alpha)$, where $m^*$ is the mass of an incoming particle in region I and $\alpha$ is the constant absorption parameter. From Fig. 10, we see that the wavefunctions on either side are given by

$$\psi_I(x) = ae^{ik_I x} + re^{-k_I x},\ x < 0;$$
$$\psi_{II}(x) = te^{ik_{II} x},\ x > 0, \tag{20}$$

where the wavevector $k_I = \sqrt{2m^*E/\hbar^2}$, and $k_{II}$ is as yet undetermined. The differential wave equation satisfied by these two wavefunctions are given by

$$\frac{d^2}{dx^2}\psi_I(x) + k_I^2\psi_I(x) = 0,\ x < 0;$$
$$\frac{d}{dx}\frac{m^*}{\overline{m}}\psi_{II}(x) + k_I^2\beta\psi_{II}(x) = 0,\ x > 0, \tag{21}$$

where, the parameter $\beta$ is fixed later through the no reflection condition. Continuity of the wavefunction at the interface $x = 0$ requires that

$$a + r = t. \tag{22}$$

The probability current continuity demands that the 'mass-derivative' of the wavefunction be continuous.[8] Hence, we have the condition

$$i\frac{k_I}{m^*}(a - r) = i\frac{k_{II}}{\overline{m}}t. \tag{23}$$

From Eq. (22) and (23), the reflection coefficient is given by

$$r = a\left(\frac{k_I\overline{m} - k_{II}m^*}{k_I\overline{m} + k_{II}m^*}\right), \tag{24}$$

and the no reflection condition is

$$k_{II} = \frac{\overline{m}}{m^*}k_I = (1 + i\alpha)\ k_I. \tag{25}$$

Substituting Eq. (20) in Eq. (21), we obtain the dispersion relation of the form

$$-\frac{m^*}{\overline{m}}k_{II}^2 + \beta k_I^2 = 0. \tag{26}$$

Hence we obtain, $\beta = (1 + i\alpha)$. In practice, we consider the absorption parameter $\alpha$ to increase smoothly over the stealth region. Therefore, the wave equation in the stealth region is given by

$$-\frac{\hbar^2}{2m^*}\frac{d}{dx}\left(\frac{1}{(1 + i\alpha(x))}\frac{d}{dx}\psi(x)\right) - E(1 + i\alpha(x))\psi(x) = 0, \tag{27}$$

with solutions of the form

$$\psi(x) \sim \exp\left(\pm ik_I x - k_I\int_0^{\pm x} dx'\alpha(x')\right). \tag{28}$$

Thus there are no sharp interfaces or jump conditions anywhere to generate any reflections. We see that the solutions are highly damped which allows us to put Dirichlet BCs at the boundaries of stealth regions. The probability current continuity requires that the absorption function $\alpha(x)$ be a smooth function. In this paper, we choose $\alpha(x)$ to be cubic Hermite interpolation polynomials which vary from 0 to $\alpha_{max}$ within the stealth region. The width of the stealth region and $\alpha_{max}$ are optimized in such a way that the sum of reflection $(R)$ and transmission $(T)$ coefficients is closest to 1 up to a desired accuracy. In the absence of a scatterer, this procedure determines these parameters in a convenient manner.

## REFERENCES


(1) M. L. Goldberger and K. M. Watson, *Collision Theory* (J. Wiley and Sons, NY, 1964).

(2) J. J. Sakurai, *Modern Quantum Mechanics* (Addison-Wesley, Reading, MA, 1994).

(3) D. Bohm, *Quantum Theory* (Dover, NY, 1989).

(4) L. R. Ram-Mohan, *Finite Element and Boundary Element Applications in Quantum Mechanics* (Oxford U.P., Oxford, UK, 2002).

(5) Jianming Jin, *The Finite Element Method in Electromagnetics* (3rd ed.) (Wiley-IEEE Press, Hoboken, NJ, 2014).

(6) P. F. Bagwell, Phys. Rev. B. **41**, 15, 10354–10357 (1990).

(7) U. Fano, Phys. Rev. **124**, 1866–1878 (1961).

(8) D. BenDaniel and C. Duke, Phys. Rev. **152**, 2, 683 (1966).